JCTC Journal of Chemical Theory and Computation

# Modeling DNA Dynamics under Steady Deforming Forces and Torques

Alexey K. Mazur

*CNRS UPR9080, Institut de Biologie Physico-Chimique, 13, rue Pierre et Marie Curie, Paris 75005, France*

Received March 16, 2009

**Abstract:** An algorithm is developed for modeling atom-level dynamics of DNA subjected to steady external torques. For completeness, simulations with steady stretching loads are also considered. The algorithms were tested in Brownian dynamics simulations of discrete wormlike chain models with calibrated elastic properties to confirm that the elastic responses induced are of desired type and magnitude and that no side effects appear. The same methods were next used in a series of 100-ns all-atom MD simulations of tetradecamer DNA fragments with explicit water and counterions. The results demonstrate the possibility of probing regular elastic responses in DNA under low, nearly physiological amplitudes of forces and torques.

## Introduction

Many fundamental biological processes are governed by the complex mechanics of the double-stranded DNA (dsDNA).[1] The dsDNA is very stiff compared to other polymers,[2,3] and yet all its known X-ray structures are irregular and can be considered as deformed double helixes.[4,5] The deformations are attributed to specific base pair sequences, crystal packing forces, bound proteins, and so forth, indicating that the DNA double helix responds noticeably to any external perturbation, suggesting that this response is elastic. The conditions in the living cell are still more severe because the dsDNA is densely packed in chromosomes and forced to bend, twist, and stretch by numerous protein factors responsible for regulation of all vital processes.[6,7] The stressed double helix, therefore, represents a major interest for experimental and theoretical investigations. In recent years, the nanomanipulation techniques made possible twisting and stretching of single dsDNA molecules using calibrated external forces and torques.[8] These experiments provided rigorous tests of theories of polymer elasticity and further increased the theoretical interest of this field by revealing unforeseen phenomena like structural transitions under extreme stress and the coupling between small torsion and stretching deformations.[9,10] Some results of these studies are controversial, notably, the nature of the overstretching transition[11,12] and the measured value of the torsional stiffness.[2,13]

The foregoing problems represent a major challenge for atom-level molecular modeling which, in principle, can trace the effects of mesoscopic external stress in the detailed structure and dynamics of dsDNA. Already the pioneering computational studies of dsDNA probed its deformations using energy minimization in implicit solvent with bending potential restraints.[14] Since then the power of computational methods gradually increased owing to improvement of force fields[15−17] and simulation techniques.[18] Modern free molecular dynamics (MD) simulations produce realistic conformational ensembles of dsDNA,[19] which makes possible modeling of the stressed double helix with thermal fluctuations taken into account. In several recent investigations, restraining potentials were applied in the course of MD simulations to measure the free energies of strongly deformed states obtained by stretching,[20,21] twisting,[22,23] and bending[24] of dsDNA. Such use of conservative restraining forces follows the classical paradigm of molecular simulations,[25] but in some cases it would be advantageous to consider instead the DNA subjected to a steady stress. For instance, according to experiment, the torsional stiffness of circular dsDNA noticeably changes with small untwisting as a result of supercoiling.[26] One can use all-atom MD for measuring the torsional stiffness of short DNA,[27,28] but to reproduce the conditions inside a supercoiled plasmid, a steady torque should be applied from both ends. Using potential restraints in this case is difficult, albeit possible. Importantly, simulations with steady forces and torques correspond to the most common experimental conditions in vitro; therefore, the computed thermodynamic averages would be directly com-

10.1021/ct900124n CCC: $40.75 
Published on Web 07/01/2009

parable to experiment without differentiation of free energy profiles. An additional technical advantage is that one does not need to care about the absolute values of geometric parameters corresponding to different DNA lengths and sequences.

In the present article we describe and test an algorithm for modeling atom-level dynamics of dsDNA subjected to steady external torques. Simulations with steady stretching loads are considered as well, which is necessary for completeness because in experiments twisting and stretching are usually applied together. Steady stretching of dsDNA can also be modeled by using anisotropic pressure control.[29] To make sure that our algorithms induce elastic responses of desired type and magnitude and do not cause side effects, we first checked these methods in Brownian dynamics (BD) simulations of discrete wormlike chain (WLC) models of calibrated elasticity. The elastic parameters of DNA and the volume of sampling in these tests were chosen to be similar to those in atomistic simulations. These results were compared with two series of 100-ns all-atom MD simulations of tetradecamer DNA fragments with explicit water and counterions. Clear deviations from the WLC behavior were observed in MD in good agreement with earlier computations and experiments. Although very slow relaxation processes apparently take place in atomistic simulations, our results demonstrate the possibility of probing regular elastic responses with low, nearly physiological amplitudes of forces and torques.

## Theory and Methods

**Algorithms for Applying Steady Stress.** The main idea of the algorithms described below is to load selected DNA bases with a set of external forces designed to cause the necessary deformation and then apply reactions to other bases to zero the total external force and torque. The technical difficulties are greatly reduced if the forces are applied to rigid Cartesian frames bound to the DNA structure, which is achieved by using virtual particles as shown in Figure 1. Four particles $X_0-X_3$ are added to purine and pyrimidine bases as shown in Figure 1 for cytosine and guanine. A rigid Cartesian frame is centered at particle $X_0$, with 1-Å distances $X_0X_i$ ($i = 1, 2, 3$) and right angles between the corresponding vectors that define three orthogonal axes. The virtual particles are used only for applying external forces; they do not take part in other interactions. Some of them overlap with real atoms, others do not. Particle $X_0$ is placed close to the center of the canonical B-DNA, with vector $X_0X_3$ approximately parallel to the helical axis. To this end, $X_1$ coincides with N1 for purines and N3 for pyrimidines, vector $X_0X_1$ points along the exterior bisector of the corresponding planar angle, and the Cartesian frame is rotated around $X_0X_1$ to put $X_2$ in the plane of the base, with vector $X_0X_3$ pointing in a 5′ to 3′ direction in B-DNA.

Construction of dsDNA fragments is illustrated in Figure 2a. The modified bases are placed at the 3′ ends of the two strands, with $X_0X_3$ vectors pointing in the opposite exterior directions. Modified versions of the four standard bases are needed for modeling arbitrary base pair sequences. In the subsequent derivations we assume that the Cartesian frame is rigid and forms a united rigid body with the base. This is natural for the internal coordinate molecular dynamics (ICMD) method we use for DNA simulations.[30,31] In the context of standard Newtonian dynamics these algorithms can be adapted with appropriate constraints and/or harmonic restraints applied to the virtual particles.

Consider a dsDNA fragment sketched in Figure 2b. We denote vectors $X_iX_j$ and the corresponding unit vectors as $\mathbf{r}_{ij}$ and $\mathbf{e}_{ij}$, respectively. Vectors $\mathbf{e}_{03}$ and $\mathbf{e}_{0'3'}$ continue the

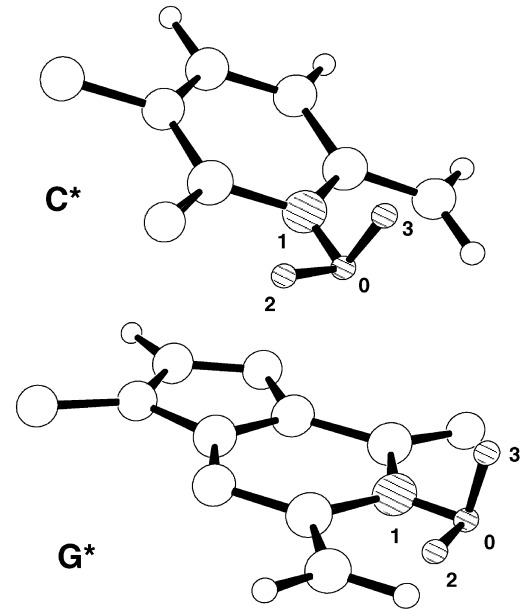


***Figure 1.*** Construction of rigid local coordinate frames at nucleobases using virtual particles. Positions of the virtual particles are shown by dashed balls for cytosine and guanine. Similar modifications are applied to adenine and thymine. The perspective drawings were produced with ORTEP.[53]

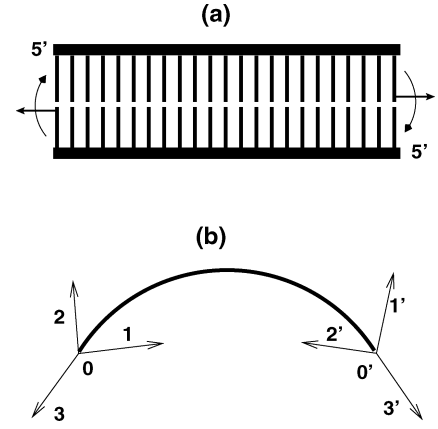


***Figure 2.*** Construction of dsDNA with modified bases displayed in Figure 1. (a) A ladder schema of a dsDNA fragment of 23 bp. Modified bases are placed at the 3′ ends of each strand. The arrows indicate the orientations of the terminal coordinate frames and the possible directions of applied torques. (b) The schema used for illustration of torques applied to curved DNA. The thick line represents the trace of a dsDNA fragment. The two terminal Cartesian frames are shown by vectors with the axes marked by the corresponding numbers of virtual particles. The right-hand frame is primed for distinction.

double helix in the two opposite directions. A torque $\mathbf{T}$ around vector $\mathbf{e}_{03}$ is created by a couple applied to particles $X_0$ and $X_2$. A steady force of magnitude $\tau$ acts on $X_0$ along vector $\mathbf{e}_{01}$ and an opposite force acts on $X_2$. The resulting torque is $\mathbf{T} = \tau\mathbf{e}_{03}$. This vector can be decomposed into a component $\mathbf{T}_{\|}$ parallel to vector $\mathbf{r}_{00'}$ and a perpendicular component denoted as $\mathbf{T}_{\perp}$. We have

$$\mathbf{T}_{\|} = \mathbf{e}_{00'}(\mathbf{T}\cdot\mathbf{e}_{00'}) = \tau\mathbf{e}_{00'}(\mathbf{e}_{03}\cdot\mathbf{e}_{00'})$$

and

$$\mathbf{T}_{\perp} = \mathbf{T} - \mathbf{T}_{\|}$$

Component $\mathbf{T}_{\perp}$ is compensated by a reaction couple applied to particles $X_0$ and $X_0'$. Its value $f_{00'}$ and direction $\mathbf{e}_{\perp}$ are obtained as

$$f_{00'} = \tau|\mathbf{e}_{03} - \mathbf{e}_{00'}(\mathbf{e}_{03}\cdot\mathbf{e}_{00'})|/|\mathbf{r}_{00'}|$$

and

$$\mathbf{e}_{\perp} = \pm(\mathbf{e}_{03}\times\mathbf{e}_{00'})/|\mathbf{e}_{03}\times\mathbf{e}_{00'}|$$

When vectors $\mathbf{e}_{03}$ and $\mathbf{e}_{00'}$ are collinear, these reactions are unnecessary and $f_{00'} = 0$.

Component $\mathbf{T}_{\|}$ is projected onto vectors $\mathbf{e}_{0'1'}$, $\mathbf{e}_{0'2'}$, and $\mathbf{e}_{0'3'}$ and compensated by three reaction couples applied to particles $X_{0'}-X_{3'}$. For instance, the component along vector $\mathbf{e}_{0'3'}$ can be compensated by forces applied to $X_{0'}$ and $X_{2'}$ parallel to $\mathbf{e}_{0'1'}$ with magnitudes

$$f_{0'2'} = \pm(\mathbf{e}_{0'3'}\cdot\mathbf{T}_{\|})$$

The other two reaction couples are computed similarly. One can choose between several alternative ways of applying these reactions, which does not affect the results. In principle, the original torque $\mathbf{T}$ could be directly projected onto the opposite coordinate frame and compensated by reaction couples applied to its axes. With some orientations, however, these reactions would correspond to bending rather than twisting. The decomposition into $\mathbf{T}_{\|}$ and $\mathbf{T}_{\perp}$ reduces the magnitudes of undesirable nontwisting reactions applied to the molecule.

By construction, the foregoing operations result in zero total force and torque on the DNA fragment. Since the individual forces are applied at different points, internal stress and deformations are introduced that should correspond to overall twisting. It is instructive to consider some extreme cases. If $\mathbf{e}_{03}$ and $\mathbf{e}_{0'3'}$ are antiparallel as in straight or circular DNA, $\mathbf{T}_{\perp} = 0$, the original couple and its torque are compensated by $f_{0'2'} = \tau$, and we obtain pure torsional stress. In contrast, when $\mathbf{e}_{03}$ and $\mathbf{e}_{0'3'}$ are parallel as in a U-turn, the original torque is completely compensated by $f_{00'}$, with no reactions applied to the primed coordinate frame. In this case rotation of the dsDNA fragment around its curved axis does not affect the total angular momentum and becomes a kind of internal degree of freedom. The external torque appears to be opposed only by solvent friction; therefore, the kinetic energy would be pumped into the system, leading to a temperature explosion. To reduce the probability of such situations, the external stress is applied symmetrically; that is, two torques of $0.5\tau$ are applied from the opposite DNA ends and compensated as described above.

The same terminal coordinate frames were used for other types of external stress. A steady stretching load was created by two opposite forces of magnitude $f$ along vector $X_0X_{0'}$. Bending stress can be obtained similarly to twisting by changing the direction of the original torque $\mathbf{T}$ so that the corresponding couple would be applied to particles $X_0$ and $X_3$ in a locally fixed plane. The case of bending strain was not studied here because it is mainly relevant to protein−DNA interactions, which involves essential complications that go beyond the present study.

**Brownian Dynamics.** The behavior of dsDNA consistent with the WLC theory[3,32] was simulated by Brownian dynamics of a composite-bead chain described in a recent report.[28] Every base pair was represented by a rigid composite bead of four virtual particles labeled $P_0^i-P_3^i$ that form a rigid Cartesian frame similar to those in Figure 1. The upper index refers to the consecutive bead number in the chain. The total energy of an $N$-bead chain is composed of bond stretching, torsion, and bending terms as

$$U = \frac{h}{2}\sum_{i=1}^{N-1}(l_i - l_0)^2 + \frac{q}{2}\sum_{i=1}^{N-1}(\phi_i - \phi_0)^2 + \frac{g}{2}\sum_{i=1}^{N-2}\theta_i^2 \quad (1)$$

All other interactions between the beads can be neglected because we consider only short stiff chains that cannot loop. Here, $l_i$ is the distance between particles $P_0^i$ and $P_0^{i+1}$ and $l_0$ is its equilibrium value. The $l_0$ value was 0.35 nm, corresponding to one base pair step. The torsion potential was applied to dihedral angles $\phi_i = P_1^iP_0^iP_0^{i+1}P_1^{i+1}$, with the equilibrium helical twist angle $\phi_0 = 0$ used for convenience. In the bend energy term, the angular displacement was measured for angles $\theta_i = P_0^iP_0^{i+1}P_0^{i+2}$.

The DNA elasticity is conveniently characterized by three persistence lengths (PLs) corresponding to bending, twisting, and stretching that we denote here as $l_b$, $l_t$, and $l_s$, respectively. Parameters $g$, $q$, and $h$ in eq 1 were chosen so that the PL values were similar in BD and MD. The energy coefficients were first estimated analytically and then verified by processing the resulting BD trajectories with previously described procedures.[28,33] For bending and twisting we applied $l_b$ = 73 nm and $l_t$ = 137 nm. The stretching PL is difficult to measure accurately.[28] Here, we used $l_s$ = 100 nm corresponding to the Young's modulus $Y_f$ = 1410 pN. The average DNA length and the overall winding were evaluated from the corresponding instantaneous values as $\langle L = \sum_{i=1}^{N-1} l_i\rangle$ and $\langle\Phi = \sum_{i=1}^{N-1}\phi_i\rangle$, respectively, where the angular brackets denote time averaging. These values are appropriate for discussing macroscopic elastic responses. Note also that the fluctuations of $\langle L\rangle$ and $\langle\Phi\rangle$ in real DNA cannot be obtained by averaging base-step parameters because of the near-neighbor correlations. The bending is conveniently characterized by parameter $\langle 1 - \cos(\Theta)\rangle$ where angle $\Theta$ was measured between vectors $X_0X_3$ and $X_{0'}X_{3'}$.

The BD simulation algorithm was considered in detail in a previous report.[28] It is based on earlier results of different groups.[34−38] For better comparison with atom-level MD, we

considered short chains of 14 composite beads, computed BD trajectories of 100 ns with a time step of 0.005 ps, and saved chain configurations every 5 ps. The reduced time step removed a small discrepancy between the measured and the analytical values of the torsional PL and improved the even distribution of torsional fluctuations within the chains.

**Molecular Dynamics.** The classical MD simulations were carried out using previously described protocols.[27,28] The starting states were prepared as follows. A tetradecamer DNA fragment with the canonical B-DNA conformation[39] was immersed in a 6.2-nm cubic cell with a high water density of 1.04. The box was neutralized by placing $Na^+$ ions at random water positions at least 5 Å from the solute. The system was energy minimized and dynamics were initiated with the Maxwell distribution of generalized momenta at low temperature. The system was next slowly heated to 293 K and equilibrated for 1.0 ns. After that, the water density was adjusted to 0.997 by removing the necessary number of water molecules selected randomly at least 5 Å from DNA and ions, and the simulations were continued with NVT ensemble conditions. The temperature was maintained by the Berendsen algorithm[40] applied separately to DNA, water, and ions, with a relaxation time of 10 ps. Simulations with external forces and torques started from equilibrated states after a few nanoseconds of free dynamics.

The AMBER98 force field parameters[15,16] were used with the rigid TIP3P water model.[41] The electrostatic interactions were treated by the SPME method,[18] with the common values of Ewald parameters, that is, 9-Å truncation for the real space sum and $\beta \approx 0.35$. To increase the time step, MD simulations were carried out by the ICMD method,[42,43] with the internal DNA mobility limited to essential degrees of freedom and rotation of water molecules and internal DNA groups including only hydrogen atoms slowed down by weighting of the corresponding inertia tensors.[44,45] The double-helical DNA was modeled with all backbone torsions, free bond angles in the sugar rings, and rigid bases and phosphate groups. The effect of these constraints is insignificant, as was previously checked through comparisons with standard Cartesian dynamics.[27,44] The time step was 0.01 ps and the DNA structures were saved every 5 ps. All trajectories were continued to 100 ns and the sampled conformations of the double helix were analyzed by program 3DNA.[46]

In all MD simulations we used the tetradecamer AT-alternating dsDNA fragment ($d(AT)_7$). This choice is consistent with recent computations[28,33,33] and it was dictated by the following considerations. The length, slightly larger than one helical turn, is convenient for measuring the elastic parameters of DNA.[28] These molecules are homopolymers of AT units; therefore, they cannot have distinguished asymmetric structures like static bends. True homopolymer DNA duplexes have special features and, in free MD with the AMBER force field, these structures deviate from the canonical B-DNA, stronger than AT- and GC-alternating sequences.[47] The terminal AT base pairs open rather frequently during nanosecond time scale MD, which significantly perturbs the flanking DNA structure. Because this dynamics cannot be averaged during the accessible duration of MD trajectories, we blocked it by applying upper distance restraints similar to those used in NMR-based structure calculations.[48] The restraints of the following form

$$U_r(r_{ij}) = \begin{cases} A_r(r_{ij} - r_0)^2, & r_{ij} > r_0 \\ 0, & r_{ij} \le r_0 \end{cases}$$

were applied to atoms of Watson−Crick hydrogen bonds in terminal base pairs. The cutoff $r_0$ was 3.6 and 2.5 Å, respectively, for the donor−acceptor and hydrogen−acceptor distances. The value of $A_r$ was 1 kcal·mol·Å$^{-2}$ for both. Because of the relatively large $r_0$ distances, these restraints operate only during rare and short intervals when the base pairing is close to rupture. Analysis of trajectories showed that the probability of such events varied from 0.03 to 3.5% for different restraints, and that the fraction of states with nonzero restraint energy was below 7.4%. Therefore, the spurious perturbations of averages can be considered negligible.

The MD simulations with the AMBER force field were earlier shown to suffer from rare irreversible transitions of backbone torsion angles to nonstandard states, which was attributed to force field artifacts.[17,49] Analysis of our trajectories revealed a pattern of conformational substates qualitatively similar to those found in earlier studies, but the relative populations of noncanonical conformers were not as large as those in the report by Dixit et al.[49] The irreversible $\gamma^{g+} \rightarrow \gamma^{t}$ transitions accompanied by $\alpha^{g-}/\alpha^{g+}$ and $\beta^{t}/\beta^{g+}$ dynamics were observed in all the terminal ApT steps. Therefore, only the central dodecamer was chosen for the analysis. A few $\gamma^{g+} \rightarrow \gamma^{t}$ transitions within this fragment are mentioned in the Results section. Their effect was not essential for the purposes of the present study.

## Results

**Validation by Brownian Dynamics.** The artificial external stress is meant to be applied in the course of long all-atom MD simulations, with the DNA chain taking many different conformations. Correct algorithms should produce perturbations of desired type and magnitude and should not give side effects like compressing or stretching along with twisting, for instance. It is essential to check for such artifacts before application in MD; otherwise, small artificial correlations between twisting and stretching can be confused with similar properties of real DNA observed in experiments.[9,10] The BD simulations of discrete WLC models of dsDNA are well-suited for the verification tests because they correctly sample from canonical ensembles of chain configurations and also give an appreciation of convergence to be expected with durations of trajectories accessible in MD.[28,33]

The effect of the steady torsional stress on the BD of the discrete WLC model is shown in Figures 3 and 4. The DNA length is just a little longer than one helical turn, which is appropriate for probing the DNA elasticity by all-atom MD simulations.[28] Accordingly, the duration of trajectories and the elastic parameters of DNA correspond to the common MD conditions. The range of torque values covers that used in single-molecule experiments[13] as well as the range of stability of real DNA. The BD results confirm that the algorithm correctly works in these conditions and that it can

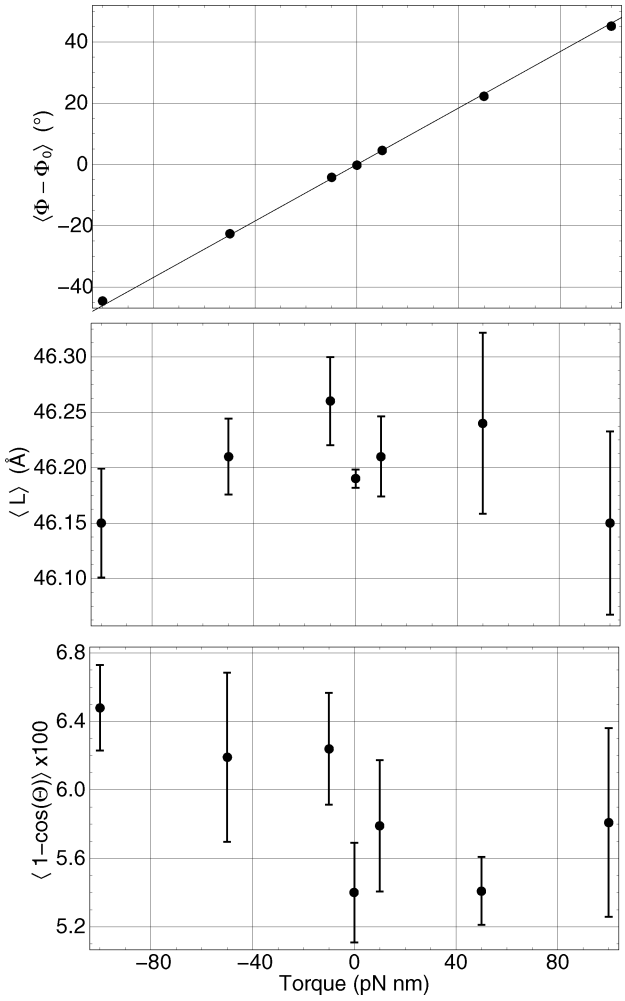


***Figure 3.*** BD simulations of DNA with applied external torques of different magnitudes. The results are shown for the overall twisting (top), DNA length (middle), and bending (bottom). The straight line on the top panel shows the theoretical dependence for $l_t = 137$ nm. The error bars show statistical errors evaluated by the method of block averages.[25] Every trajectory was divided into four equal parts (blocks) and the errors are estimated from standard deviations of the block averages. For twisting the errors are smaller than the size of the plot points.

hardly cause spurious artifacts in MD. The overall DNA winding changes linearly with the torque, in quantitative agreement with theory. The torsional stress is evenly distributed over the whole chain (see Figure 4). The DNA length is constant within the error limits. The stretching/compression side effects are negligible and indistinguishable by practical methods of measuring the length of all-atom DNA. In long DNA, the external torsional stress causes buckling transitions and here it should increase bending. Figure 3 does not contradict that, but for one DNA turn this effect is small.

Similar tests for steady stretching are shown in Figures 5 and 6. In single-molecule experiments forces up to 45 pN are used to keep DNA straight[13] and the B-DNA double helix remains stable with forces below 70 pN. It can be seen that within this range of forces the steady stretching algorithm does not cause spurious side effects. The DNA length increases in quantitative agreement with theory. The stretching stress is evenly distributed along the chain (see Figure 6). Figure 6 looks more noisy than Figure 4, even though the respective ranges of stretching and torsion deformations correspond to similar energies. This difference is due to very fast single-step torsion relaxation[28] that results in a better convergence for 100 ns of BD. The overall winding fluctuates near zero without distinguishable trends. The bending steadily decreases. Interestingly, it is reduced by less than two times and does not level even with very large forces, which means that DNA stretching always leaves some freedom for local bending.

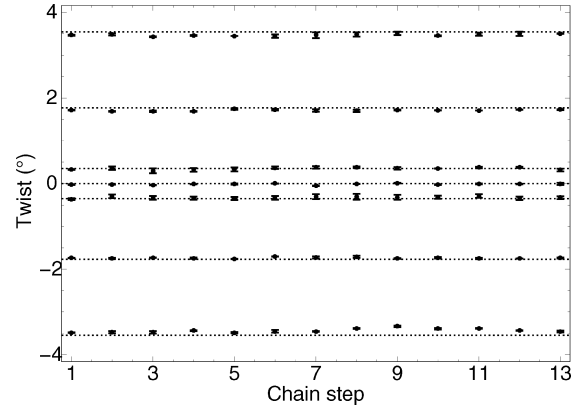


***Figure 4.*** BD simulations of DNA with applied external torques of different magnitudes. The distribution of the torsional deformations along the chain. The torque values are the same as those in Figure 3. Theoretical values corresponding to a WLC model with $l_t = 137$ nm are shown by horizontal dotted lines. The errors are similar to the size of the plot points.

**Molecular Dynamics.** The results of the MD tests are displayed in Figures 7−10. The data analysis involved the central part of a tetradecamer AT-alternating dsDNA. The choice of this specific fragment was explained in the Theory and Methods section. Regular elastic responses to twisting and stretching are shown, respectively, in the top panel of Figure 7 and the middle panel of Figure 9. The overall winding $\Phi$ exhibits linear variations with torque, in good qualitative and quantitative agreement with the WLC theory, as well as the earlier measured twisting stiffness. The $\langle L(f) \rangle$ dependence is clearly ascending as it should be, but the statistical errors are larger than those in the BD tests in Figure 5 and one can only say that the amplitude of the extension roughly corresponds to the stretching Young's modulus of 1100 pN. This parameter is intrinsically difficult to measure accurately in MD simulations of short DNA.[28]

Compared to the corresponding BD plots, MD exhibits an evidently broader scattering of points around the theoretical straight lines, indicating the presence of slow processes with relaxation times beyond those observed with the discrete WLC models. Very slow processes of still unclear nature were experimentally detected in short dsDNA.[50,51] However, a few systematic shifts of the plot points in Figures 7 and 9 correlate with, and are probably caused by, the rare $\gamma^{g+} \rightarrow \gamma^{t}$ backbone transitions (see the Theory and Methods section). An isolated transition such as this does not cause gross changes in the DNA structure, but it results in a stepwise increase of the local twist and rise and, accordingly, augments

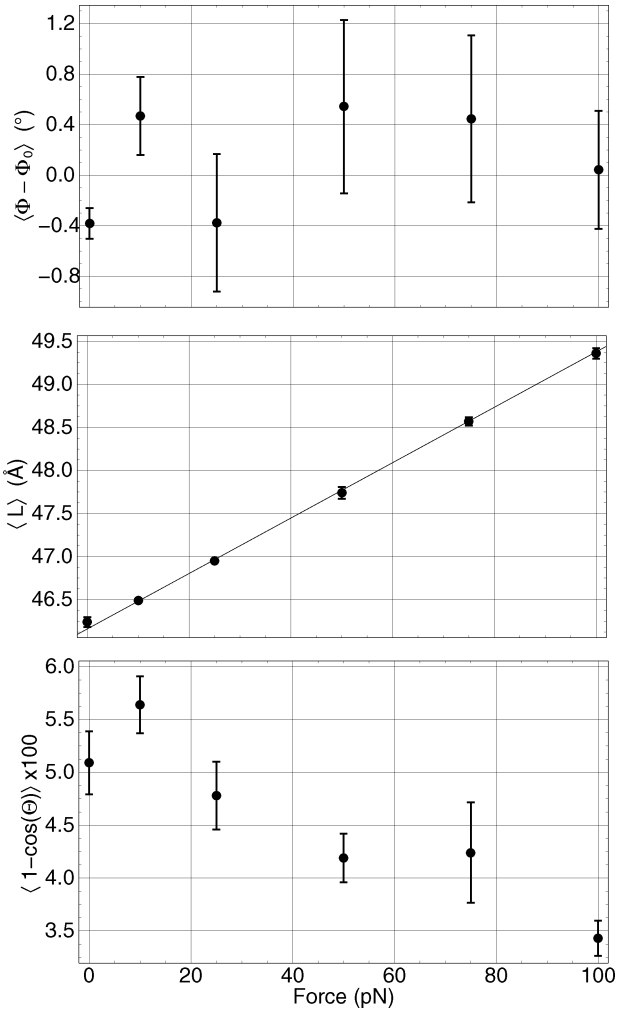


***Figure 5.*** BD simulations of DNA with applied external stretching forces of different magnitudes. The results are shown for the overall twisting (top), DNA length (middle), and bending (bottom). The straight line on the middle panel shows the theoretical dependence for $l_s = 100$ nm. In this panel, the statistical errors are similar to the size of the plot points.

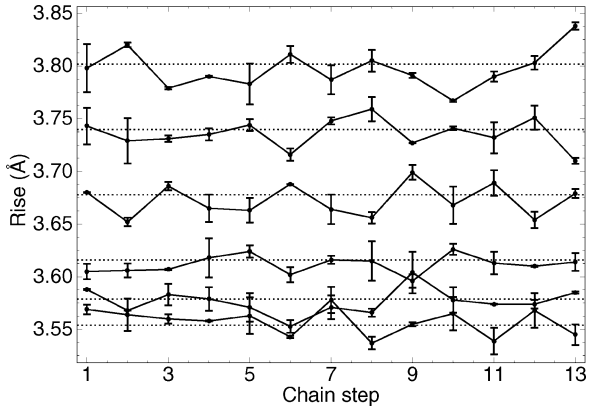


***Figure 6.*** BD simulations of DNA with applied external stretching force of different magnitudes. The distribution of the stretching deformations along the chain. The force values are the same as those in Figure 5. The horizontal dotted lines mark the theoretical levels corresponding to $l_s = 100$ nm.

the measured overall DNA length and winding. In Figure 7, for instance, no $\gamma^{g+} \rightarrow \gamma^{t}$ transitions occurred with zero and

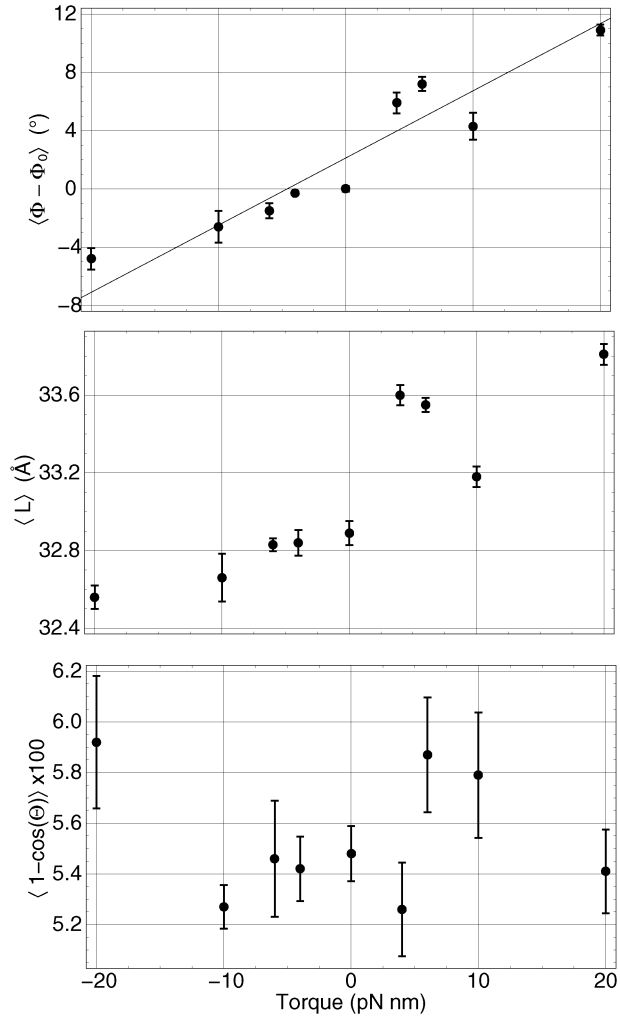


***Figure 7.*** MD simulations of DNA under external twisting torque of different magnitudes. The results are shown for the overall twisting (top), DNA length (middle), and bending (bottom). The straight line on the top panel shows the theoretical dependence for $l_t = 137$ nm.

negative torques. With $\tau = 10$ pN two isolated transitions occurred, but they reversed after about 30 and 60 ns, respectively. Finally, in each of the trajectories with $\tau = 4$, 6, and 20 pN one nonreversed transition took place. These rare events evidently correlate with the small shifts of the plot points in Figure 7. The stretching data were affected by three isolated nonreversed $\gamma^{g+} \rightarrow \gamma^{t}$ transitions. One of them occurred with $f = 10$ pN, but it happened late in the dynamics and did not cause noticeable effects. The other two transitions took place during dynamics under 4 pN stretching, and the corresponding data points are clear outliers (see Figure 9).

The above rare conformational transitions do not hide the regular trends produced by the applied external stress. The middle panel of Figure 7 shows the chiral effect revealed in single-molecule experiments,[9,10] namely, that the DNA length is increased with overtwisting and reduced with unwinding. The pattern in Figure 7 is qualitatively different from that in Figure 3, which proves that this subtle feature is not a mere artifact. With a torque of 20 pNnm, the increase in the DNA length extrapolated from experimental data[9] should be around 0.14 Å, which agrees reasonably well with Figure 7. No statistically significant trends could be detected

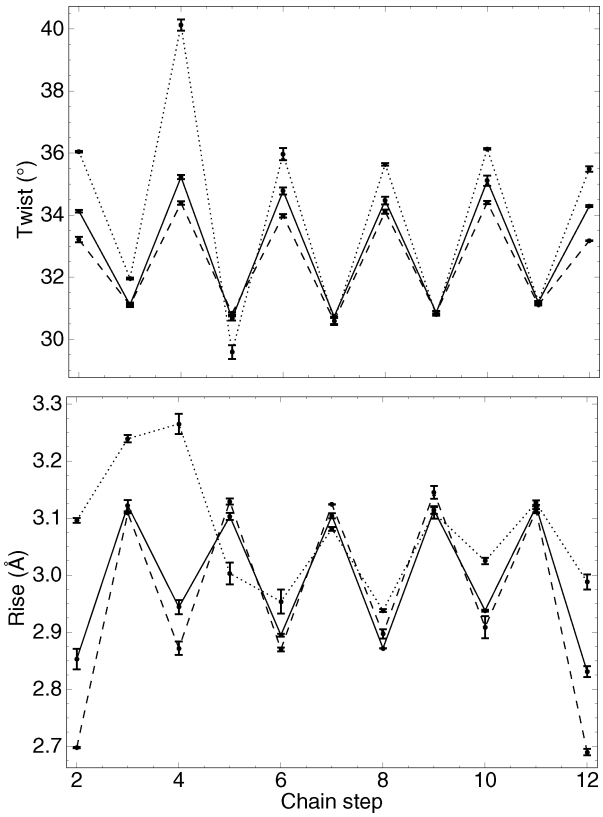


***Figure 8.*** MD simulations of DNA under external twisting torque of different magnitudes. Distribution of perturbations along the chain for twisting (upper panel) and stretching (lower panel). The torque values are 0 pN·nm (solid line), −20 pN·nm (dashed line), and +20 pN·nm (dotted line).

for bending, which qualitatively agrees with the BD data (compare the bottom panels of Figures 7 and 3).

Figure 8 demonstrates that the external torque is evenly distributed over the double helix. The ApT and TpA steps are characterized by strongly different values of equilibrium intrinsic twist and rise. The figure shows that the TpA steps are much more receptive to forced twisting than the ApT steps. This agrees with earlier experimental and computational observations.[5,22] In simulations with the overtwisting torque of 20 pN·nm the fourth TpA step exhibited anomalous behavior because of a $\gamma^{g+} \rightarrow \gamma^{t}$ transition in one of the strands. This transition changes the equilibrium intrinsic twist, which corresponds to plastic (nonelastic) deformability, but it can also affect the local stiffness. The noncanonical $\alpha/\gamma$ backbone conformations are considered as force field artifacts in free MD simulations, but such conformers are frequent in protein−DNA complexes.[52] The anomalous stiffness of such conformers may be important for biology and this issue deserves future study. The lower panel in Figure 8 demonstrates also that the lengths of the terminal base pair steps are affected by external twisting stronger than others.

The results of MD simulations with steady external stretching are analyzed in Figures 9 and 10. With the stretching load most common for experiments ($f < 20$ pN)[9,13] only small perturbations of the DNA structure and dynamics are distinguishable. The chiral twist−stretch coupling revealed in the middle panel of Figure 7 should result in

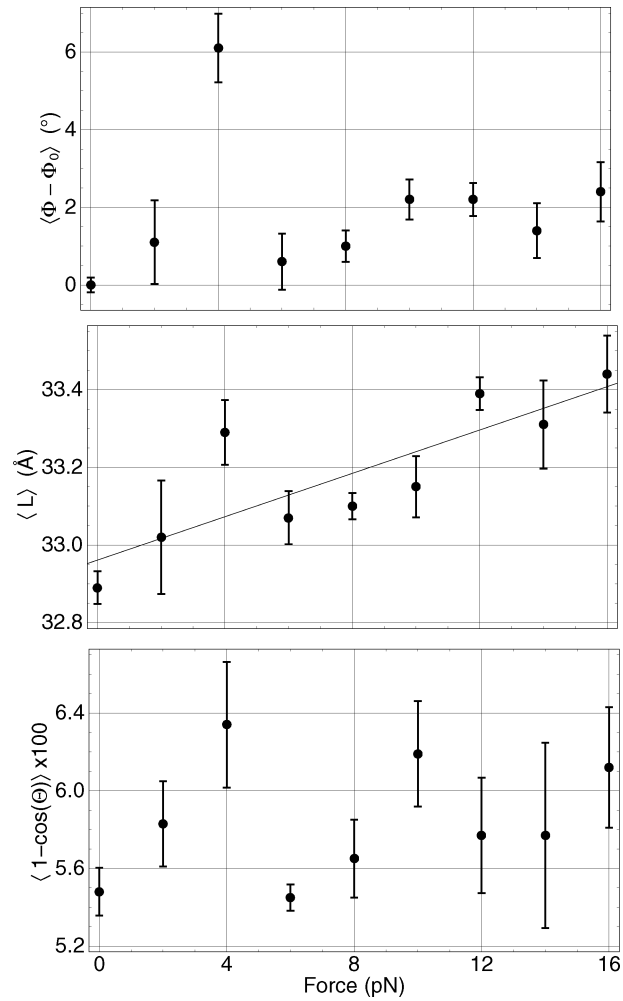


***Figure 9.*** MD simulations of DNA under external stretching force of different magnitudes. The results are shown for the overall twisting (top), DNA length (middle), and bending (bottom). The straight line on the middle panel shows the best fit theoretical dependence corresponding to $l_s = 83$ nm ($Y_f = 1170$ pN).

overwinding with increased force. According to experiment,[9] for the stretching load of 16 pN, the $\Delta\Phi$ value should reach ca. 0.6°. Our results do not contradict this estimate (cf. top panel of Figure 9), but the effect is within the amplitude of statistical fluctuations and smaller than the shift at 4 pN caused by two $\gamma^{g+} \rightarrow \gamma^{t}$ transitions mentioned above. It might be generally difficult do detect such small change with the DNA length accessible in MD because the sign of the coupling is apparently inverted with forces beyond 20 pN.[9] The bottom panel of Figure 9 exhibits bending fluctuations comparable with the corresponding plate in Figure 5 for BD. The perturbations produced by external stretching are evenly distributed along the double helix (Figure 10). Similarly to Figure 8 the TpA steps are noticeably more susceptible to deformations than the ApT steps. In contrast, the terminal base pair steps do not show excessive deformability as those shown in Figure 8; moreover, they seem to be more rigid than the internal steps.

## Discussion

This article presents a nonstandard approach to modeling deformed states of dsDNA. Replacing potential geometric

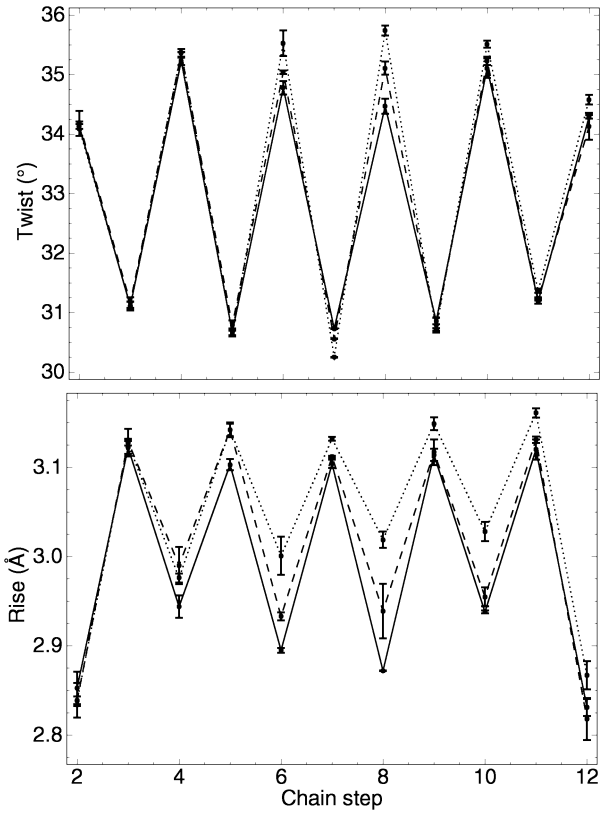


***Figure 10.*** MD simulations of DNA under external stretching force of different magnitudes. Distribution of perturbations along the chain for twisting (upper panel) and stretching (lower panel). The force values are 0 pN·nm (solid line), 8 pN (dashed line), and 16 pN (dotted line).

restraints by nonpotential forces and torques is analogous to the switch from constant volume to constant pressure simulations of continuous media. The steady stress conditions correspond to the state of short dsDNA fragments in living cells and also in single-molecule experiments. To my knowledge, the present study is the first such attempt. Methods of this type will serve as a useful supplement to the earlier setups using potential restraints and umbrella sampling.[20−22,24]

Steady forces are seldom used in MD simulations because it is difficult to anticipate situations where the system appears outside domains of attraction and dynamics become unbound. One relevant example was considered above in the derivation of the steady torque algorithm. The possibility of other potentially dangerous configurations cannot be excluded for long dsDNA. Our tests demonstrate that the algorithms proposed are sufficiently robust for small DNA lengths and the values of torques and forces corresponding to experimental and physiological conditions. I believe, however, that the same approach can be safely applied to somewhat longer dsDNA, notably, that it can be used for modeling the buckling transition in medium length fragments. Such studies are planned.

The results of MD simulations reported here are preliminary. They confirm the correctness of the algorithms and the principal possibility of imitating the steady stress conditions in all-atom MD of dsDNA. These computations are continued to obtain a more representative sampling and to check the possible effect of the external stress on the elastic parameters of dsDNA. Additional longer simulations are planned to probe such effects for other biologically relevant base pair sequences. Despite the above limitations, the results reported here illustrate the power of modern MD methods; notably, we demonstrated that atomistic simulations can reproduce linear elastic response of dsDNA in quantitative agreement with the WLC theory and the elastic parameters previously evaluated by other methods. The present data also give an appreciation of the complexity and the richness of real DNA dynamics compared to the discrete WLC models and BD simulations.

An important technical problem in long-time MD simulations of dsDNA is related to rare noncanonical backbone transitions.[49] The number of such events here was less significant than might be expected, and moreover, in two cases reverse transitions occurred. This can be attributed to (i) the use of AMBER98 rather than other similar force field versions and (ii) a fortunate choice of the base pair sequence. Free AMBER simulations are known to underestimate the helical twist in dsDNA, but this effect is less pronounced for some sequences and it was specifically reduced by the AMBER98 force field modifications.[16] The overall shift of the dsDNA structure toward the A-form may favor the noncanonical backbone transitions. Future simulations should use the recently improved force field version[17] to reduce the probability of such events. However, the noncanonical backbone conformations are observed in protein−DNA complexes;[52] therefore, the properties of these conformers should be studied as well.

Traditional approaches using potential restraints and umbrella sampling are designed to improve the sampling of weakly populated states; therefore, they facilitate probing strong DNA deformations. For small perturbations considered here these methods are not efficient because the shifts in the restrained values would be smaller than the natural thermal fluctuations. In such cases, the potentials of mean force (PMF) can be obtained from a single unrestrained computation. However, very high accuracy of the PMF profile is necessary for extracting the first and second derivatives required for the evaluation of the elastic parameters of DNA and comparisons with experiment. In the published umbrella sampling calculations[20−22] the PMFs obtained were below the noise level in the range of forces and torques considered here. At the same time, a number of intriguing features in the biological function of dsDNA involve very small changes in the helical twist, for instance. The steady stress algorithms are specifically designed for probing such conditionsl therefore, they should find many interesting applications.

## References

(1) Bloomfield, V. A.; Crothers, D. M.; Tinoco, I. *Nucleic Acids. Structures Properties and Functions*; University Science Books: Sausaliito, CA, 2000.

(2) Hagerman, P. J. *Annu. Rev. Biophys. Biophys. Chem.* **1988**, *17*, 265–286.

(3) Cantor, C. R.; Schimmel, P. R. *Biophysical Chemistry, Part III: The Behavior of Biological Macromolecules*; W.H. Freeman: San Francisco, 1980.

(4) Dickerson, R. E. In *Oxford Handbook of Nucleic Acid Structure*; Neidle, S., Ed.; Oxford University Press: New York, 1999; pp 145−197.

(5) Olson, W. K.; Gorin, A. A.; Lu, X. J.; Hock, L. M.; Zhurkin, V. B. *Proc. Natl. Acad. Sci. U. S. A.* **1998**, *95*, 11163–11168.

(6) Widom, J. *Q. Rev. Biophys.* **2001**, *34*, 269–324.

(7) Cozzarelli, N. R.; Cost, G. J.; Nollmann, M.; Viard, T.; Stray, J. E. *Nat. Rev. Mol. Cell. Biol.* **2006**, *7*, 580–588.

(8) Bustamante, C.; Bryant, Z.; Smith, S. B. *Nature* **2003**, *421*, 423–427.

(9) Gore, J.; Bryant, Z.; Nollmann, M.; Le, M. U.; Cozzarelli, N. R.; Bustamante, C. *Nature* **2006**, *442*, 836–839.

(10) Lionnet, T.; Joubaud, S.; Lavery, R.; Bensimon, D.; Croquette, V. *Phys. Rev. Lett.* **2006**, *96*, 178102.

(11) Cluzel, P.; Lebrun, A.; Heller, C.; Lavery, R.; Viovy, J. L.; Chatenay, D.; Caron, F. *Science* **1996**, *271*, 792–794.

(12) Rouzina, I.; Bloomfield, V. A. *Biophys. J.* **2001**, *80*, 882–893.

(13) Bryant, Z.; Stone, M. D.; Gore, J.; Smith, S. B.; Cozzarelli, N. R.; Bustamante, C. *Nature* **2003**, *424*, 338–341.

(14) Zhurkin, V. B.; Lysov, Y. P.; Ivanov, V. I. *Nucleic Acids Res.* **1979**, *6*, 1081–1096.

(15) Cornell, W. D.; Cieplak, P.; Bayly, C. I.; Gould, I. R.; Merz, K. M.; Ferguson, D. M.; Spellmeyer, D. C.; Fox, T.; Caldwell, J. W.; Kollman, P. A. *J. Am. Chem. Soc.* **1995**, *117*, 5179–5197.

(16) Cheatham, T. E., III; Cieplak, P.; Kollman, P. A. *J. Biomol. Struct. Dyn.* **1999**, *16*, 845–862.

(17) Perez, A.; Marchan, I.; Svozil, D.; Sponer, J.; Cheatham, T. E.; Laughton, C. A.; Orozco, M. *Biophys. J.* **2007**, *92*, 3817–3829.

(18) Essmann, U.; Perera, L.; Berkowitz, M. L.; Darden, T.; Lee, H.; Pedersen, L. G. *J. Chem. Phys.* **1995**, *103*, 8577–8593.

(19) Cheatham, T. E., III; Kollman, P. A. *Annu. Rev. Phys. Chem.* **2000**, *51*, 435–471.

(20) MacKerell, A. D., Jr.; Lee, G. U. *Eur. Biophys. J.* **1999**, *28*, 415–426.

(21) Harris, S. A.; Sands, Z. A.; Laughton, C. A. *Biophys. J.* **2005**, *88*, 1684–1691.

(22) Kannan, S.; Kohlhoff, K.; Zacharias, M. *Biophys. J.* **2006**, *91*, 2956–2965.

(23) Wereszczynski, J.; Andricioaei, I. *Proc. Natl. Acad. Sci. U. S. A.* **2006**, *103*, 16200–16205.

(24) Curuksu, J.; Zakrzewska, K.; Zacharias, M. *Nucleic Acids Res.* **2008**, *36*, 2268–2283.

(25) Frenkel, D.; Smit, B. *Understanding Molecular Simulations. From Algorithms to Applications*; Academic Press: New York, 1996.

(26) Selvin, P. R.; Cook, D. N.; Pon, N. G.; Bauer, W. R.; Klein, M. P.; Hearst, J. E. *Science* **1992**, *255*, 82–85.

(27) Mazur, A. K. *Biophys. J.* **2006**, *91*, 4507–4518.

(28) Mazur, A. K. *J. Phys. Chem. B* **2009**, *113*, 2077–2089.

(29) Luan, B.; Aksimentiev, A. *Phys. Rev. Lett.* **2008**, *101*, 118101.

(30) Mazur, A. K. *J. Am. Chem. Soc.* **2000**, *122*, 12778–12785.

(31) Mazur, A. K. *J. Am. Chem. Soc.* **2002**, *124*, 14707–14715.

(32) Landau, L. D.; Lifshitz, E. M. *Statistical Physics, Part 1*; Nauka: Moscow, 1976.

(33) Mazur, A. K. *J. Phys. Chem. B* **2008**, *112*, 4975–4982.

(34) Ermak, D. L.; McCammon, J. A. *J. Chem. Phys.* **1978**, *69*, 1352–1360.

(35) Allison, S. A. *Macromolecules* **1986**, *19*, 118–124.

(36) Iniesta, A.; de la Torre, J. G. *J. Chem. Phys.* **1990**, *92*, 2015–2018.

(37) Chirico, G.; Langowski, J. *Macromolecules* **1992**, *25*, 769–775.

(38) Jian, H.; Schlick, T.; Vologodskii, A. *J. Mol. Biol.* **1998**, *284*, 287–296.

(39) Arnott, S.; Hukins, D. W. L. *Biochem. Biophys. Res. Commun.* **1972**, *47*, 1504–1509.

(40) Berendsen, H. J. C.; Postma, J. P. M.; van Gunsteren, W. F.; DiNola, A.; Haak, J. R. *J. Chem. Phys.* **1984**, *81*, 3684–3690.

(41) Jorgensen, W. L.; Chandreskhar, J.; Madura, J. D.; Impey, R. W.; Klein, M. L. *J. Chem. Phys.* **1983**, *79*, 926–935.

(42) Mazur, A. K. *J. Comput. Chem.* **1997**, *18*, 1354–1364.

(43) Mazur, A. K. *J. Chem. Phys.* **1999**, *111*, 1407–1414.

(44) Mazur, A. K. *J. Am. Chem. Soc.* **1998**, *120*, 10928–10937.

(45) Mazur, A. K. *J. Phys. Chem. B* **1998**, *102*, 473–479.

(46) Lu, X.-J.; Olson, W. K. *Nucleic Acids Res.* **2003**, *31*, 5108–5121.

(47) Mazur, A. K. *J. Chem. Theory Comput.* **2005**, *1*, 325–336.

(48) Kozin, S. A.; Bertho, G.; Mazur, A. K.; Rabesona, H.; Girault, J. P.; Haertle, T.; Takahashi, M.; Debey, P.; Hoa, G. H. *J. Biol. Chem.* **2001**, *276*, 46364–46370.

(49) Dixit, S. B.; Beveridge, D. L.; Case, D. A.; Cheatham, T. E., III; Giudice, E.; Lankas, F.; Lavery, R.; Maddocks, J. H.; Osman, R.; Sklenar, H.; Thayer, K. M.; Varnai, P. *Biophys. J.* **2005**, *89*, 3721–3740.

(50) Brauns, E. B.; Madaras, M. L.; Coleman, R. S.; Murphy, C. J.; Berg, M. A. *Phys. Rev. Lett.* **2002**, *88*, 158101.

(51) Sen, S.; Andreatta, D.; Ponomarev, S. Y.; Beveridge, D. L.; Berg, M. A. *J. Am. Chem. Soc.* **2009**, *131*, 1724–1735.

(52) Varnai, P.; Djuranovic, D.; Lavery, R.; Hartmann, B. *Nucleic Acids Res.* **2002**, *30*, 5398–5406.

(53) Burnett, M. N.; Johnson, C. K. *ORTEP-III: Oak Ridge Thermal Ellipsoid Plot program for crystal structure illustrations*; Oak Ridge National Laboratory Report ORNL-6895; Oak Ridge National Laboratory: Oak Ridge, TN, 1996.

CT900124N